BPF-LIKE ANTENNA VALIDATION IN AN UWB IN-CAR WIRELESS CHANNEL

Journal:	*IET Communications*
Manuscript ID:	COM-2014-0057.R3
Manuscript Type:	Research Paper
Date Submitted by the Author:	08-Oct-2014
Complete List of Authors:	Garcia Zuazola, Ignacio; University of Deusto, Faculty of Engineering Sharma, Ashwani; University of Deusto, Faculty of Engineering Whittow, William; Loughborough University, Electronic and Electrcial Engineering Elmirghani, J. M. H.; University of Leeds, School of Electronic and Electrical Engineering Batchelor, John; University of Kent at Canterbury, Electronic Engineering Laboratory
Keyword:	WAVE PROPAGATION, ANTENNA TESTING, MICROWAVES

BPF-LIKE ANTENNA VALIDATION IN AN UWB IN-CAR WIRELESS CHANNEL

I.J. Garcia Zuazola[1,3*], L. Azpilicueta[2], A. Sharma[1], H. Landaluce[1], F. Falcone[2], I. Angulo[1], A. Perallos[1], W.G.Whittow[5], J.M.H. Elmirghani[3], J.C. Batchelor[4]

[1]Deusto Institute of Technology, University of Deusto, Avenida de las Universidades 24, 48007 - Bilbao, Spain
[2]Department of Electronics, Public University of Navarra, Pamplona, Navarra, Spain
[3]School of Electronic and Electrical Engineering, University of Leeds, Leeds, LS2 9JT, UK
[4]Department of Electronics, University of Kent, Canterbury, Kent CT2 7NT, UK
[5]School of Electronic, Electrical and Systems Engineering, Loughborough University, Loughborough, Leicestershire, LE11 3TU, UK
**Email: igarcia@theiet.org*

Abstract:

Ultra-wide band (UWB) is a very attractive technology for innovative in-car wireless communications requiring high data rates. A designated antenna, which presents a reflection coefficient (S11) matched band comparable to the Band Pass Filters (BPF) normally required at the transducers, plays a positive contribution in this in-car application and was validated for the scenario. The inherited BPF-like response of the antenna relaxes the specification of the front-end BPF components of the transceivers. The in-car propagation channel was modelled and used to validate the BPF-like antenna. For the modelling, a comprehensive set of well-defined measurements (using a standard antenna) were used to set-up the in-car channel simulator and simulated results were used to validate the BPF-like antenna. Additionally, the performance of the UWB radio system is studied and the probability of errors over the communication channel compared using the standard and the BPF-like antenna by predictions.

1 Introduction

UWB technology can potentially deliver high data rate and spatial capacity, with low power / low cost designs and multipath immunity [1]. This wireless technology inside vehicles provides connectivity and mobility to a host of passenger devices while allowing the potential reduction of the costs and weight of the electrical wiring.

In this paper, a previously published antenna design [2] fits in this UWB radio system. The designated antenna presents a matched S11 band comparable to that of the BPF normally required at the transducer, allowing for a relaxed specification of the BPF components at the front-end; hereby termed as BPF-like antenna. The in-car propagation channel was analytically modelled in Section 2, and corroborated using previously published measurements [1] of the genuine in-car scenario using a standard antenna from Wisair Ltd. Since predictions agreed to measurements, Section 3, potential antenna candidates can be validated by simulation, without engaging in new measurements; therefore avoid extensive hardware preparations. To validate the BPF-like antenna in the in-vehicle scenario (which uses an IEEE 802.15 MB- OFDM system for its relative immunity to Gaussian noise [3]), the radio propagation performance of the UWB radio system is studied and the accuracy of the data transmissions made by comparing the results to those obtained using the standard antenna. The channel model assumes a descriptive in-car scenario of a motionless vehicle with windows, without occupants and considers damping materials (dielectric constant and permittivity). This is a reasonable assumption and predictions using this model are valid for determining whether new antennas (the BPF-like antenna) are suitable for the in-car application. In addition, it provides a prospective insight of the performance in-car.

In essence, the in-car channel model relied on previously measured results using the standard antenna to approve the simulator and consequently validate the BPF-like antenna by simulations (compared to those of the standard); this is the reason why once the simulator was

conveniently established, the non-need of re-measuring the channel using the BPF-like antenna. Similarly, we aim to validate the BPF-like antenna for the in-car scenario, rather than claiming outperformance over the standard.

2 In-car system set-up

Based on a practical scenario, the geometry of a Renault Extra Van [1], Fig. 1, is used for experimentation. In this work, rather than finding unknown models for in-car communications we validate the BPF-like antenna for the in-vehicle scenario.

In [1], a DV9110 Development Kit (DVK) from Wisair Ltd, based on MB-OFDM technology, was used. The set-up used two UWB transceivers; one was used as an access point (AP) and the other as mobile equipment (ME). In this work, the AP used the standard and the BPF-like antennas interchangeably, Section 3, and emitted *"a short pulse of output power of 80μW [power spectral density (PSD) of -42 dBm/MHz max] containing the WiMedia / MBOA group 1 sub-band (3.168 – 4.752GHz) and using a modulated signal MB-OFDM (QPSK)"* as in [1].

The experimental measurements (presented in Section 3) using the standard antenna (a monopole of 2 dBi gain [1] measured at the Half Power BeamWidth (HPBW)) were used to characterise the analytical model; a three dimension (3D) Ray Launching simulator based on Matlab and complemented by Agilent Advanced Design System (ADS) schematics.

For the wireless propagation channel, we considered a radius, r = 0.9m, Fig. 1b, and the AP was set in the middle of the ceiling of the car since this was *"the preferred location in vehicles to ensure a good power distribution to likely ME locations within the car"* [1].

Therefore, the antennas (AP and ME) were located as shown in Fig. 1b, where the horizontal distance, r, between the AP antenna and the front panel is 0.9m and the height of the AP antenna above the ME is 0.8m; "*the most likely location for the ME/fixed equipment in this setting"* [1].

In isolation, the antennas have omni-directional patterns and both antennas present similar radiation patterns in the elevation plane (E-plane) and the azimuth plane (H-plane); this is presented in Section 3. The standard antenna was 4cm away from the ceiling of the car to preserve impedance matching; the BPF-like antenna was adequate for as low as 1cm separation from the ceiling.

The BPF-like antenna, introduced in Section 3.1 favours the application in effectively guiding Electromagnetic (EM) waves inside the vehicle while eluding those emanating outside the fuselage of the vehicle; this is achieved by radiating uniformly in the plane perpendicular to the antenna while minimising those in the rear direction (backward). In addition, this considerably benefits for the settlement of antennas in close proximity to the (steel-made) ceiling of the car. For this reason, the desired main beam of the antenna in this setting is preferred in the radiation pattern (in polar) form of 270^{o} to 90^{o}, meaning that any null happening in the 90^{o} to 270^{o} range is satisfactory; this is because "ideally", pattern truncations (from 90^{o} to 270^{o}) favours the application.

The presented work is aimed to first define the simulator by comparing uniquely the simulated vs. measured channel responses using the standard antenna and then to carry-on the evaluation of the antennas via simulations. That means, the BPF-like antenna is only

compared to the standard version by simulation. The personalized simulator allows for the validation of the BPF-like antenna without extensive/additional experimental set-ups.

The calibration of the simulator (based on the approximation of radio wave propagation inside the vehicle) was made by reasonable agreement between the measured and simulated in-car responses using the standard antenna. The model incorporates graphical information of the in-vehicle scenario for the predictions, assessment and validation of the BPF-like antenna, and uses antenna radiation patterns in 3D for the evaluation.

Subsequently, the characteristics of the UWB peer-to-peer links within the vehicle were analysed using both antennas (standard and BPF-like). For evaluation purposes, this included the channel temporal characteristics: delay spread (DS) and amplitudes of multipath signals; path loss (PL); spatial/spectral capacities; and bit error rate (BER) for several conceivable non-line of sight (NLOS) scenarios. Conclusions and future work are presented in Section 4.

3 Measurements and results

Initially, the characteristic performance of the standard and BPF-like antennas are presented and evaluated. Subsequently, the simulator is validated (by reasonable agreement of the simulated vs. measured in-car channel responses using the standard antenna) and the quality degradation of travelling signals within the vehicle analysed and results presented. An assessment is performed to validate the BPF-like antenna by simulations.

3.1 The BPF-like and the standard antennas

A Planar Inverted-F Antenna (PIFA) with an input match designed to offer the capability of a front-end BPF [2], Fig. 2, is utilised in this application and referred to as BPF-like antenna.

The insertion coefficient (S21) of a commercially available UWB BPF is also shown for comparison purposes. The cut-off responses (measured at -5.2dB S11) are prominent for the BPF-like antenna and indicate the potential removal of the front-end BPF typically encountered in transceivers; since the antenna (which acts as a BPF) radiates/accepts radio waves in resonance while stopping unwanted radio waves out of resonance.

The BPF-like antenna, whose total volume dimensions are 19.58 x 15.75 x 5.53 mm, operates in the unlicensed lower band (3.168-4.752 GHz) of the UWB communication standard with a 3.57:1 voltage standing wave ratio (VSWR). The standard antenna, whose total volume dimensions are 39 x 28.8 x 0.9 mm, operates in the unlicensed lower UWB band with a 2.75:1 VSWR – these specifications are given for the stand-alone antennas in isolation. Further details of the main characteristics of the antennas are given in Table 1.

Fig. 2 shows the S11 of the standard and the BPF-like antennas. The bandwidth of the BPF-like antenna measured at the -5.2dB and this S11 is equivalent to a transfer power of 42.15%; that is a lower 0.58dB transmission coefficient for the BPF-like antenna (the standard is 1.65dB) and presents no impediment for its usage in the application. The radiation patterns of the antennas (standard and the BPF-like) in polar form are shown in Figs. 3a and 3b respectively. Although radiation patterns are frequency dependent, only small variations were observed for those resonating within the antenna´s bandwidth and only those at 4.752 GHz are included for brevity. The patterns of the BPF-like antenna are confined more effectively inside the vehicle. The immediately reported affirmations will be corroborated throughout the remaining parts of the paper.

In essence, because the BPF-like antenna utilises the car ceiling as a reflector (denoted as plane A, Fig. 1b), higher gains are achieved, Table 1. This compensates for the higher (deprived) VSWR of the BPF-like antenna.

Figs. 3a and 3b measure the radiation patterns of the antennas with/without the plane A, which dimension is 510x800x0.75mm^3, and Figs. 3c and 3d, the patterns comparison in the E- and H-planes. Because the reflector (plane A) is not electrically connected to the antenna and the relatively large size present, the effect on the patterns when attaching the antenna to the car ceiling is insignificant [1] since minor spillover (radiation falling outside the edge of the plane) is probable.

Unlike the standard antenna, the BPF-like antenna possesses a radiation pattern with better front-to-back ratio (Figs. 3c and 3d) for advanced energy confinement within the vehicle while minimizing the waves leaving the rear of the vehicle and with acceptable impedance matching in close proximity to the plane A, see Fig. 2.

Although the BPF-like antenna presents a constrained VSWR compared to that of the standard antenna (Table 1), it allows for the removal of the BPFs that are encountered immediately preceding the antenna in a transceiver, Fig. 4, and therefore adds a +2dB to the system link budget in both directions of communication. The 2dB is the measured S21 of the BPF shown in Fig. 2. Because of the +2dB compensation and the lower 0.58dB transmission coefficient for the BPF-like antenna (previously outlined), the transfer power of the BPF-like antenna is evidently improved by 1.42dB (compared to the standard antenna) when the BPF is present. Therefore, the 5.2dB S11 BPF-like antenna is valid and in addition, this antenna has the capability of being 3cm closer to the plane A without compromising its performance;

compared to the standard version, that is 1cm for the BPF-like antenna and 4cm for the standard antenna.

Although the pattern of the BPF-like antenna was perceived beneficial (higher gains in the desired direction), this was not solely the important element for the application. Compared to the S11 response of the commercially available BPF, Fig. 2, the BPF-like antenna S11 is narrower in BW and therefore slightly improves rejection of the spectrum outside the actual BW. With a removed BPF, the BPF-like antenna provides comparable S11 performance to that of the commercial BPF and any possible spectrum beyond the antenna cut-off response (S11 = 0dB) is rejected by the amplifier´s inherent BW response.

To compare the practice of the antennas fairly, unlike the BPF-like antenna, the standard antenna requires the BPF in place. Because the S11 of the former is -5dB and the latter -10dB, only when the BPF is in place, limits the link budget S21 by an inherent 2dB insertion loss of the filter, lower overall performance and is comparable to the BPF-like antenna for its validation in-car.

3.2 The channel simulator

Popular and reliable prediction models based on empirical analysis, such as the COST 231, Walfish-Bertoni, and Okumura Hata, have been widely used for the approximation of radio wave propagation in different scenarios due to its relatively fast-processing [4-6]. Nevertheless, they rely on previously measured channel models incorporating graphical information of the scenario for optimum predictions, and unless a precise calibration is made (using regression methods), inaccurate propagation models are conducted.

For more accurate solutions, deterministic models are preferred [7-12]. They use a numerical approach for the solving of Maxwell's equations, e.g. ray launching and ray tracing or full wave simulation techniques, such as the Method of Moments (MoM), Finite-difference time-domain (FDTD), and Finite-integration time-domain (FITD). These methods are highly precise, but do require inherent computational complexity and extensive time-processing.

A more balanced solution for the propagation prediction of highly diffractive coefficients and offering a reasonable trade-off between accuracy and computational time is reported based on geometrical optics [13].

For the assessment of the in-vehicle channel impairments using the antennas, the quality degradation of transmitting signals inside the vehicle are analysed using the 3D ray launching method; an algorithm primarily based on the electric field and refractive coefficients of traveling signals [14] implemented in Matlab. The in-house algorithm accounts for the complex nature of the in-vehicle scenario and includes the following considerations; frequency of operation, graphical resolution, separation angle between adjacent rays, number of multipath reflections and transmit power, Table 2, the antenna radiation patterns in 3D, the in-vehicle geometry (Fig. 1b), and damping materials including the windows permittivity (ε_r) of 6.06 and conductivity (σ) of 10^{-12} [S/m].

The reflection, refraction and diffraction coefficients of the radio waves are considered; this is the refractive index of the scenario (n = ~1), including the dielectric constant and the loss tangent. The cuboids resolution was set to 10cm to balance accuracy with simulation time.

Using the implemented Ray Launching simulator, the standard and BPF-like antennas were individually simulated. Initially, the radiation patterns of the antennas were previously measured, in isolation and when in close proximity to the plane A. The antennas were placed to maintain impedance matching from the car body at the coordinates (x = 0.9m, y = 0.45m, z = 0.04m) and (x = 0.9m, y = 0.45m, z = 0.01m) respectively for the standard and the BPF-like antennas, Fig. 1b; that means, the BPF-like antenna resulted 3cm closer to the plane A and that translated into a more compact antenna implementation. Subsequently, the antenna patterns in 3D were imported in the simulator whose validation was effectively made by reasonable agreement between the measured and simulated responses using the standard antenna – this established the simulator for additional comparisons made exclusively by simulation (BPF-like vs. standard).

3.3 Signal strength and propagation loss

Results using the 3D Ray Launching simulator are now presented. The simulator considers the in-vehicle channel impairments using damping materials at 3.8GHz. Figs. 5a and 5b depict the power distribution of the UWB transmitter, using the standard and the BPF-like antennas, at likely ME locations within the car, z = 0.8m (Fig. 1b). The antennas were horizontally polarised and with the orientations given in Figs. 1 and 3, where the 0º of the patterns in Fig. 3 indicate the Z direction of the antennas. For the ME reception, an omnidirectional antenna was used to measure both antennas under test (AUT), was linearly horizontal polarised and had a 0dBi gain.

Observations suggest that for this AP antenna orientation and preferred location (Section 2), the distributed power within the car is improved when using the BPF-like antenna (Fig. 5b),

and provides a good insight to validate the design for this application – supplementary results will corroborate this affirmation.

A realistic comparison between the power strength levels (amplitudes) achieved by the antennas is given in Fig. 6a when the ME antenna was at r = 0 to 0.9m (Fig. 1b), and intervals of 0.1m. The small-scale fading is attributed to multipath induced fading since vehicle bodies are predominately made of steel (Fig. 1) and shows in Fig. 6b, a relatively slow fading - ripples are due to car fuselage resonances. This cannot, in principle, be attributed to shadow fading since no obstacles (i.e. passengers), except those arising from the multiple signals traveling inside the channel, were considered in the simulation.

In addition, the amplitude measured at 3.8GHz by a spectrum analyser using the standard antenna is included in the figure (Fig. 6a). The simulated and measured results using the standard antenna present reasonable agreement to validate the 3D Ray Launching simulator and set the base for the predictions – the BPF-like antenna is therefore validated via simulations.

3.4 Channel path loss

The simulated PL (attenuation of the radiated wave) at 3.8GHz of the link for the in-car scenario using the standard and the BPF-like antennas is presented in Fig. 6b when the ME antenna was at r = 0 to 0.9m (Fig. 1b), and intervals of 0.1m. Observations suggest that the existing multipath propagation contributed positively with reduced signal attenuation (9dB at 0.9m) to the channel response when using the BPF-like antenna. This is as a result from the higher 3.3dBi peak gain of the BPF-like antenna (Table 1), since it benefited from the collective resolving of more multipath components.

In addition, the measured PL using the standard antenna is included in Fig. 6b and was collected by employing a vector network analyser (VNA), where the VNA dynamic range was 80 dB and all cables and losses were removed by calibration [1]. The maximum channel PL measured at 3.8 GHz, where the antennas were considered as part of the channel, was 33.53 dB [1]. Although there is an existing 2dB difference between the simulated and the measured PL of the standard antenna (defined at 0m), the reasonable agreement between the results validates the simulator and allows for the validation of the BPF-like antenna exclusively by simulations.

Using the BPF-like antenna, the simulated Power Spectral Density (PSD) of a UWB-OFDM signal showing three bands over the effective channel 3.168 - 4.752 GHz frequency band is depicted in Fig. 6c; this is used as a base for the UWB channel model in Section 3.7. A simulated -81.30 dBm noise floor was observed and an AP transmit power of -43.42 dBm [1 MHz resolution bandwidth (RB)] was used. The noise floor was 10dB higher than that observed experimentally (using the standard antenna) [1] and is attributed to the noise figure of the simulator.

The maximum (average) power achieved by the BPF-like antenna, when the ME was located at the lowest distance r = 0m, is -69 dBm (Fig. 6a), and it fell to -81 dBm at the furthest distance r = 0.9m; both ME locations are illustrated in Fig. 1b. Compared to the standard antenna, the BPF-like version provides a +7dB link gain approximately for all over the distance (Fig. 6a). In addition, because of the inherited BPF-like response of the BPF-like antenna, a +2dB can be additionally accounted for the transmission link budget of the system; this is given by the removal of the BPF (Fig. 4) which regular insertion loss was 2dB (Section

3.1). Because higher gains are not permitted at the transmitter, governed by the Federal Communications Commission (FCC) mask (Fig. 6c), amplification has to be down-compensated and that translates into energy-savings.

The channel PL is calculated from (1)

$$PL = (P_R - G_R) - (P_T + G_T) \quad (1)$$

where $(P_R - G_R)$ is the received Effective Isotropic Radiated Power (EIRP), and $(P_T + G_T)$ is the transmitted EIRP.

This gives a channel PL (using the standard antenna) of 47dB over the maximum range of 0.9m with a variation in loss of 15dB between the closest ME location and the maximum range. For the results using the BPF-like antenna (7dB improved PL compared to that of the standard antenna), any EIRP beyond the UWB standard allowance (the standard antenna in isolation complies with the FCC mask) can be utilised to relax the required amplification of the transceiver and therefore lower its overall power consumption.

The calculations from the results in Fig. 6b show agreement with those in Fig. 6a, where the simulated channel PL is 46.23 dB, and loss variation over the closest ME location and maximum range is 14 dB using the standard antenna.

3.5 Effect of the channel on UWB pulse

The simulated effect of the channel impairments on a selected part of the UWB-modulated radio pulse waveform at the receive antenna is now presented.

Using Agilent ADS, the channel impulse response in the time domain (real time) was simulated (uses the second derivative of a Gaussian pulse of width 100ps). The transceiver emits 10 consecutive pulses of output power of 80μW and a time span of 50ns; this is equivalent to 4 x 10^{-9} Joules.

Fig. 6d shows the signal decay with distance where an overall reduction of 334.7 mV was seen (using the BPF-like antenna) between the fixed reference point AP (Fig. 1b) and the furthest range of 0.9m. The original transmitted pulse is also shown for comparison. The received pulse of 77.3 mV had a delay of 940 ps and had relatively low DS; this ensures a similar received frequency from a transmitter to a receiver sampling requirement. Compared to that using the standard antenna, the pulse using the BPF-like antenna shows 0.03 ns lower delay and similar DS and amplitude. The arrival time difference is attributed to the PL, in other words, to the antenna gain contribution.

The resultant small time of flight of the signal [15] is due to the small distances inside the car. The frequency shift of the signal (decreased for the BPF-like antenna vs. the standard), Δf, is 1.09 MHz, and calculated as,

$$\Delta f = \frac{1}{\tau_s} - \frac{1}{\tau_c} \quad (2)$$

where τ_s is the time-difference (5.19ns) between the received and the transmitted pulses using the standard antenna and τ_c (5.22ns) using the BPF-like antenna.

The modelling of the UWB channel is based on the IEEE 802.15 standard and the modified Saleh-Venezuela channel model, CM2- NLOS for indoor propagation environments, with

user defined 0-4m and PL (1). The characteristics study of the channel multipath impulse response [18] uses (3), and assumes a Poisson distribution of cluster arrival times of multipath.

$$h_i(t) = X_i \sum_{l=0}^{L} \sum_{k=0}^{K} a_{k,l}^{i} \ \delta\left(t - T_l^i - \tau_{k,l}^i\right) \tag{3}$$

where $a_{k,l}^i$ are the multipath gain coefficients, T_l^i is the delay of the l^{th} cluster, $\tau_{k,l}^i$ is the delay of the k^{th} multipath component relative to the l^{th} cluster arrival time, X_i represents the log-normal shadowing, and i refers to the i^{th} realisation.

3.6 Multipath characteristics

The channel multipath propagation characteristics were evaluated using the 3D Ray Launching simulator by examining predictable path delays and power delay profiles (PDPs) for the application.

The path delay comparison between the antennas is shown in Fig. 7a. Since these delays were assessed by simulation in Section 3.5, the reason of including the measured response of the standard antenna in the figure. For the experimental result, a VNA was used for the complex response of the channel over a range of frequencies.

The readings at a reference frequency of 3.8 GHz are depicted in Fig. 7a, show an average delay of 2ns and the maximum path delay of both antennas, seen at 0.9m, are comparable.

Because of the differential delays seen at the receiver are smaller than 1/B and UWB resolves multipath components with differential delays of 133ps, neglected intersymbol interference (ISI) is foreseen [1].

3.7 Power delay profile

Employing the 3D Ray Launching Simulator, the simulated PDP using the standard antenna is plotted in Fig. 7b, and compared to the results obtained using the BPF-like antenna. Excess delay was limited to 5.8 ns in the desired distance of 0.9m. As in [1], the PDP "*had a propagation largely immune to multipath-fading because of the broadband nature of the signal"* and was attributed to reflections caused by the short distances within the vehicle. Relatively strong multipath components and reasonably large number of echoes are observed in Figs. 7b and 7c; the latter depicts a version over a superior time span exclusively for the BPF-like antenna for the case r = 0m. The simulated PDP impulse response of both antennas is depicted in Fig. 7d; for the plotting, weak echoes that were received below 5dB were ignored. Using the BPF-like antenna, a very low delay PDP is perceived from the relatively low separation of the direct path and cluster to the first fade.

As a result, the signals performance/reception in-car is enhanced when using the BPF-like antenna due to the antenna gain and therefore the signal experiences less attenuation.

A fading effect is corroborated by the number of reflections seen in the PDP. Because a typical PDP with obstructed LOS commonly has a single cluster [17], a relatively higher LOS when using the BPF-like antenna (Fig. 7d) is achieved. A higher 6.2dB received power is apparent for the BPF-like antenna and that agrees to the antenna contribution reported in Section 3.4.

The 2dB difference between the simulated and the measured PL of the standard antenna observed in Fig. 6b was attributed to the simulator amendments and contributed to a 1.4ns inferior time-delay shift compared to measurements. The maximum excess delay is now at 5.8ns (Fig. 7b), and is tolerable for the reasonable comparison of the responses of the antennas by simulation.

Multipath propagation inside the vehicle can allow for a constructive interference with more signal power to be collected, and lead to a non-time-dispersive channel with somewhat neglected ISI (Section 3.6). Consequently, the following set of BER simulations ratifies the affirmation and validates the BPF-like antenna for the in-car application.

3.8 BER

The predicted BER performance in-car is now presented. For the test-bench set-up, Fig. 8a, a regular transmitter and receiver was concatenated by a user-defined radio channel model based on the previously presented impulse response of Fig. 6d. The model considers the antennas (gain) as part of the channel and comprises the following environmental factors: the previously presented PL and PDP respectively in Figs. 6b and 7d and the propagation distance (including multipath) of 0.9m. Essentially, the received signal is correlated with a reference waveform to account for errors in the transmission. A simulated 3.94×10^{-4} BER response using the standard antenna is depicted in Fig. 8b.

Measurements using the standard antenna corroborated the simulator. For the experimental set-up, the AP and ME intercommunicated reciprocally with each other and packets of certain known length were sent over the in-car channel; the received data was analysed and recorded

as BER, Fig. 8b. A measured BER response [1] of trend 2.5 x 10^{-4} using the standard antenna was observed and shows reasonable agreement with the predicted result. This verifies the simulator, and subsequently the BPF-like antenna is validated exclusively by simulation. Compared to the simulated response using the standard antenna, the BPF-like antenna presents a relatively lower BER and extends towards error-free communications. This BER margin can allow (within the FCC mask) for fine-tuning of the Effective Radiated Power (ERP) of the transmitter, however, the BER did not significantly vary with the +9dB link gain that was obtained using the BPF-like antenna (Section 3.4), since the received power fell within the receiver sensitivity and the lower delays of signals PDP did positively impact on the BER response. The +9dB therefore can be translated into efficient power savings.

Because the BPF-like antenna presents an improved BER over the standard antenna, it is reasonable to predict somewhat higher system capacity,

$$C_{SISO} = B\ log_2(1 + SNR) \tag{4}$$

where C_{SISO} is the maximum capacity of the UWB channel in a single-input single-output (*SISO*) communication, is computed from the Shannon capacity theorem and expressed as a function of the channel bandwidth (B) and signal-to-noise ratio (*SNR*).

Since the improved BER is in fact due to a higher SNR (quality of the transmission channel), this translates positively on the system capacity (4).

4 Conclusion

This paper has focused on the validation of a BPF-like antenna in an UWB in-car wireless channel. The designated antenna allows for the elimination of the front-end BPFs immediately

preceding the antenna in a transceiver and was intended to ensure a good power distribution inside the vehicle, elude those emanating outside the car body, and benefit its settlement in close proximity to the ceiling of the car. For the validation, an in-house 3D Ray Launching Simulator based on Matlab and complemented by a full-model OFDM-UWB system based on Agilent ADS schematics was used. The simulator was first approved by comparing the simulated vs. measured channel responses using the standard antenna and consequently the BPF-like antenna was exclusively validated via simulations. That allowed for validating the new antenna without engaging in a new measurement. For the BPF-like antenna to be measured experimentally, it would imply removal of the surface-mount device (SMD) BPFs immediately preceding the antenna in the transceiver, implement a tailored transmission-line transition to replace the SMDs and perform required Electromagnetic Compatibility (EMC) tests to maintain compliance with the FCC regulations.

The quality of transmission in the UWB radio channel was enhanced when using the BPF-like antenna due to a higher link gain and therefore a less attenuated signal, a relatively lower BER that extended towards an error-free communication, and an improved BER with potential to a higher system capacity. This corresponds to a single frequency response and the possible change of the response over the entire UWB bandwidth has not been taken into consideration. However, the results provide a good insight for validating the BPF-like antenna in the scenario.

The distributed power within the car was notable and provided a +9dB link gain. However, since an ERP beyond the FCC limits is not permitted, this can be utilised to relax the required amplification of the transceiver and that translates into energy-savings.

Future research is suggested using the broadband nature of the UWB signal and aided by commercially available electromagnetic field solvers to perceive possible changes of the response over the entire UWB bandwidth.

5 Acknowledgments

This work has been part-funded by the European Union. Many thanks to Iñaki Garcia Inal (St. George´s School - Bilbao) and Yossi Kolkovich (Wisair) for the technical support.

6 References

[1] I.J. Garcia Zuazola, J.M.H. Elmirghani, and J.C. Batchelor, 'High-speed ultra-wide band in-car wireless channel measurements", *IET Communications*, Volume 3, Issue 7, pp. 1115 – 1123, July 2009
[2] I.J. Garcia Zuazola, J.C. Batchelor, J.M.H. Elmirghani,, N.J. Gomes, 'UWB PIFA Antenna for simplified transceivers', *IET Electronics Letters*, Volume 46, Issue 2, pp. 116 – 118, January 2010
[3] S.H. Kratzet, 'MB-OFDM and DS-UWB ultra-wideband design using SystemView by Elanixw', *Eagleware-Elanix App Note AN-24B*, 30 March 2005
[4] M. Hata, "Empirical formula for propagation loss in land mobile radio services", *IEEE Transactions Antennas and Propagation*, vol. 29, nº 3, pp. 317-325, 1980
[5] F. Ikegami, S. Yoshida, T. Takeuchi and M. Umehira, "Propagation factors controlling mean field strength on urban streets", *IEEE Transactions Antennas and Propagation*, vol. 32, nº 8, pp. 822-829, 1984
[6] S. Phaiboon and P. Phokharatkul, "Path loss pred iction for low-rise buildings with image classification on 2-D aerial photographs", *Progress in Electromagnetics Research*, vol. 95, pp. 135-152, 2009
[7] J. Blas, R.M. Lorenzo, P. Fernandez, E.J. Abril, A. Bahillo, S. Mazuelas, and D. Bullido, "A new metric to analyze propagation models", *Progress In Electromagnetics Research*, vol. 91, pp. 101-121, 2009
[8] G. Dimitriou, and G.D Sergiadis, "Architectural features and urban propagation", *IEEE Transactions Antennas and Propagation*, vol 54, nº 3, pp. 774-784, 2006
[9] M. Franceschetti, J. Bruck, and L.J. Schulman, "A random walk model of wave propagation", *IEEE Transactions Antennas and Propagation*, vol. 52, nº 5, pp. 1304-1317, 2004
[10] G. Kanatas, I.D. Kountouris, G.B. Kostaras, and P. Constantinou, "A UTD propagation model in urban microcellular environments", *IEEE Transactions Vehicular Technology*, vol. 46, nº 1, pp. 185-193, 1997
[11] D.J.Y. Lee, and W.C.Y Lee, "Propagation prediction in and through buildings", *IEEE Transactions Vehicular Technology*, vol. 49, nº 5, pp. 1529-1533, 2000
[12] S.Y. Tan, and H.S. Tan, "A microcellular communications propagation model based on the uniform theory of diffraction and multiple image theory", *IEEE Transactions Antennas and Propagation*, vol 44, nº 10, pp. 1317-1326, 1996
[13] M.F. Iskander, and Z. Yun, 'Propagation prediction models for wireless communication systems', *IEEE Transactions on Microwave Theory and Techniques*, Volume 50, Issue 3, pp. 662-673, March 2002
[14] F. Esparza Alfaro, et al., 'RF environment behavior modeling based on 3-D ray-tracing and neural networks to mitigate multipath in indoor position estimation", *Proc. of the SDR'10 Technical Conference and Product Exposition*, pp. 82-86, 2010
[15] V. Hovinen, M. Hamalainem, T. Patsi, 'Ultra wideband indoor radio channel models: preliminary results', *IEEE Conf. Ultra Wideband Systems and Technologies*, Baltimore, Maryland, USA, pp.75-79, May 21-23, 2002
[16] A.F. Molisch, J.R. Foerster, M. Pendergrass, 'Channel models for ultrawideband personal area networks', *IEEE Personal Communications Magazine*, Volume 10, Issue 6, pp. 14 – 21, 2003
[17] U.G. Schuster, H. Bö Lcskei, 'Ultrawideband channel modeling on the basis of information-theoretic criteria', *IEEE Transactions Wireless Communications*, Volume 6, Issue 7, pp. 2464 – 2475, 2006
[18] S. Geng, S. Ranvier, X. Zhao, J. Kivinen, P. Vainikainen, 'Multipath propagation characterization of ultra-wide band indoor radio channels', *IEEE Int. Conf. Ultra- Wideband*, pp. 11 – 15, Zurich, Switzerland, 5 – 8 September 2005

Figures

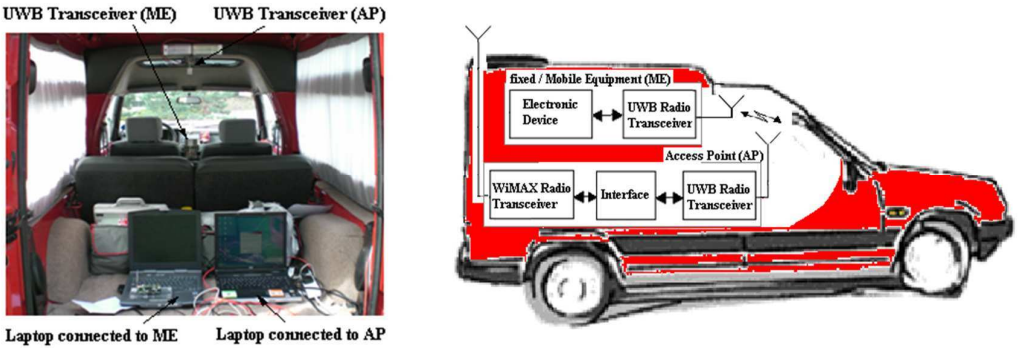

(a)

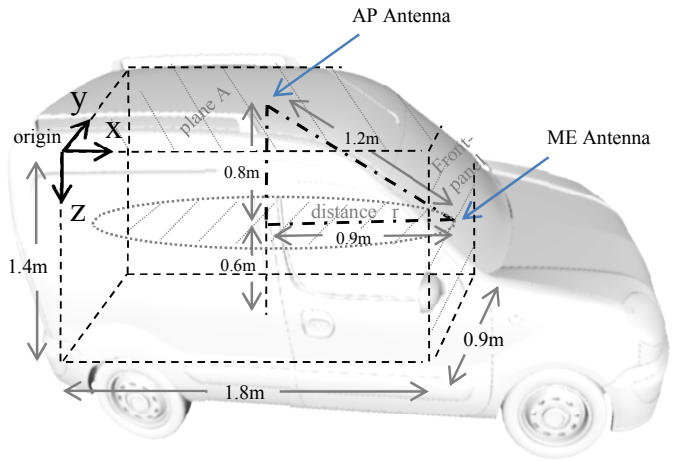

(b)

Figure 1 – (a) Experimental set-up in a typical in-car wireless channel - reproduced from [1] with permissions and (b) the in-vehicle geometry and AP location

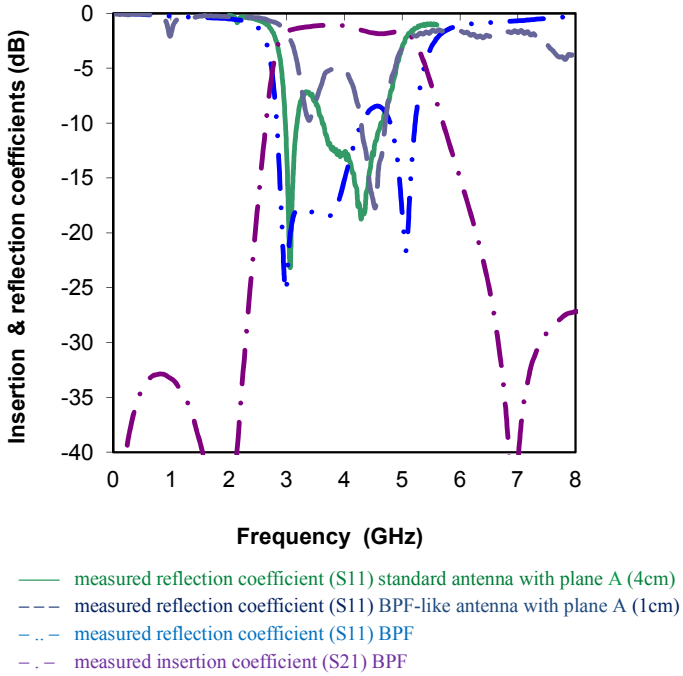

Figure 2 – The standard and the BPF-like antennas

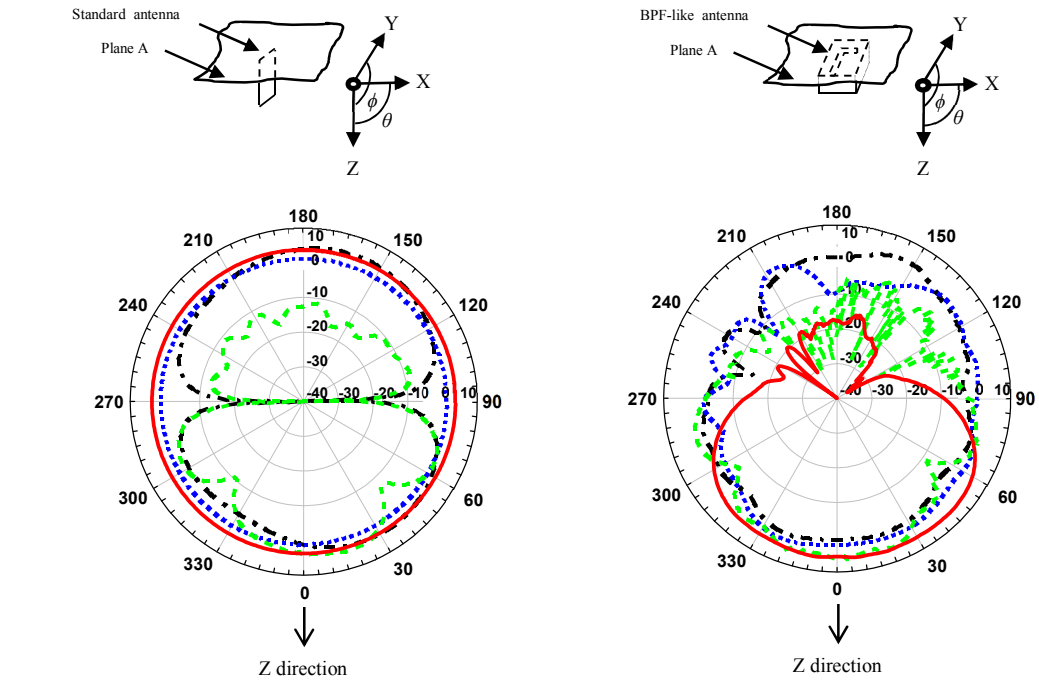

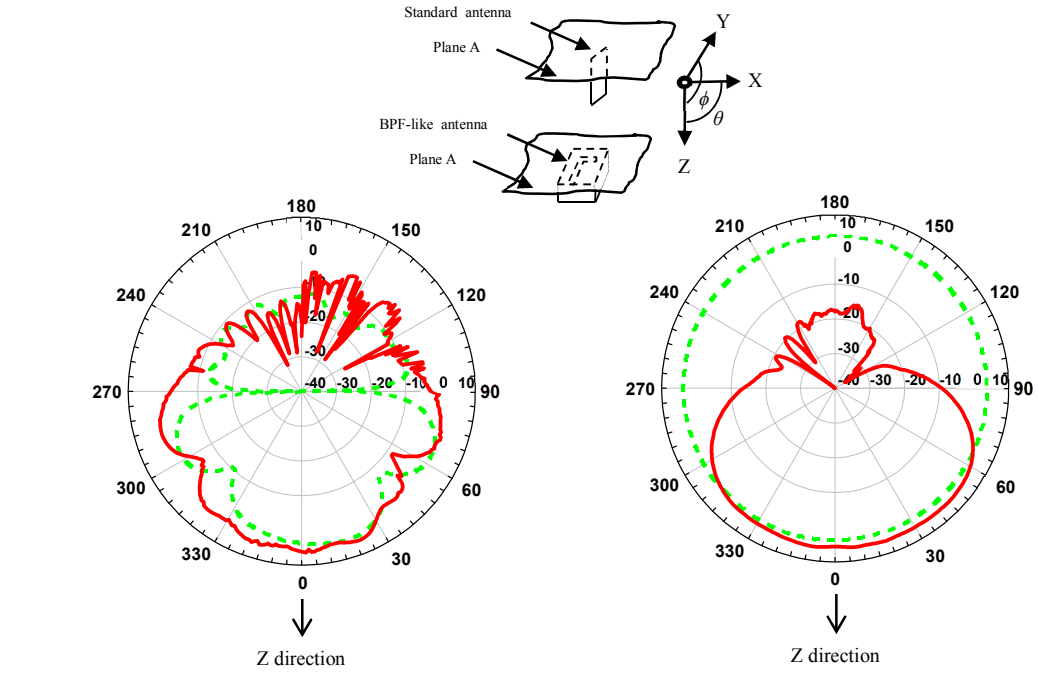

Figure 3 – Radiation patterns of (a) the standard and (b) the BPF-like antenna, and Radiation pattern comparison between the antennas (c) E-plane and (d) H-plane – absolute values in dBi

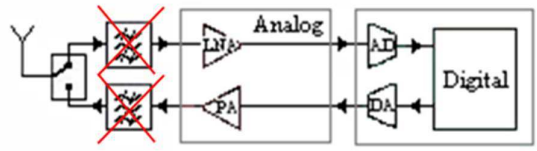

Figure 4 – Simplified UWB Transceiver

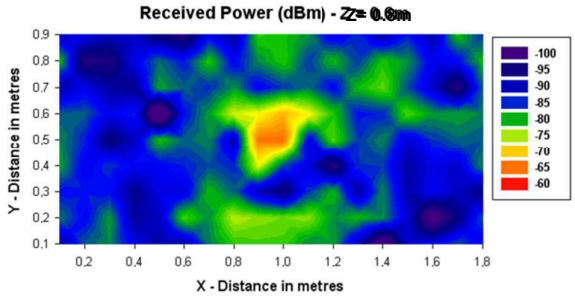

(a)

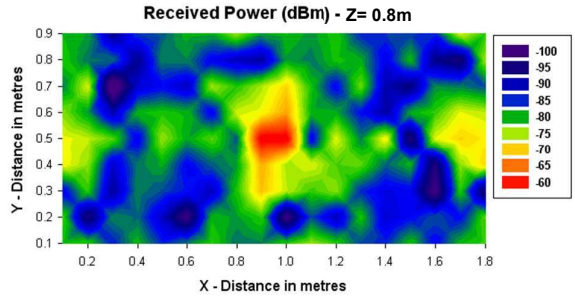

(b)

Figure 5 - Distributed power within the car using a) the standard antenna and b) the BPF-like antenna

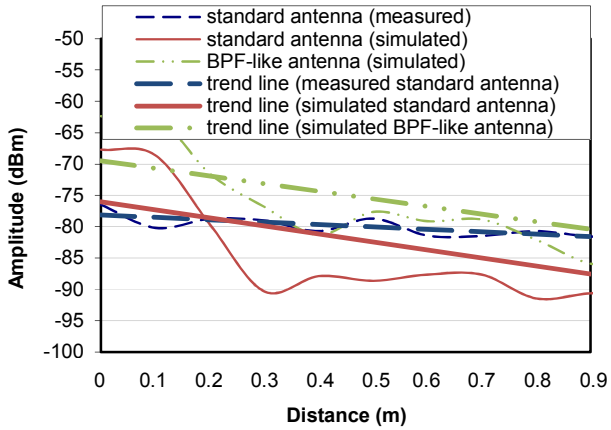

(a)

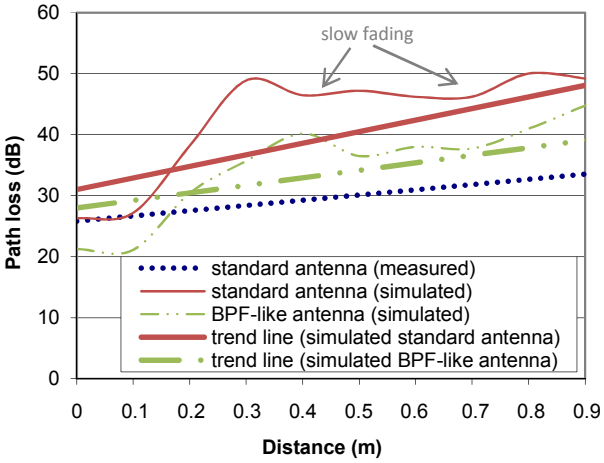

(b)

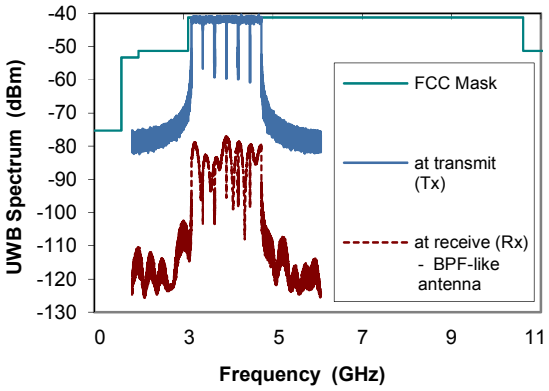

(c)

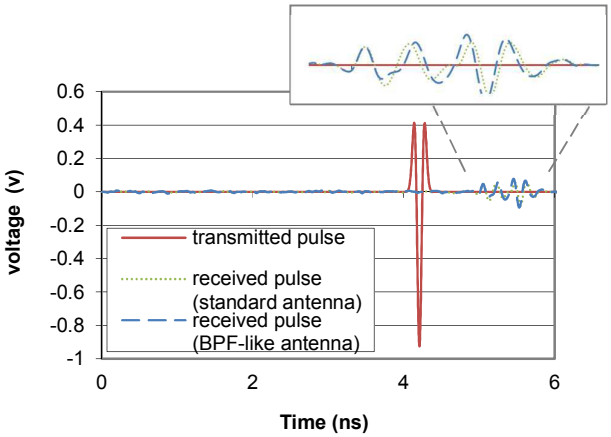

(d)

Figure 6 – (a) Simulated and measured power strength, (b) simulated and measured path loss, (c) simulated PSD, (d) simulated transmitted and received UWB pulse over the in-car wireless channel

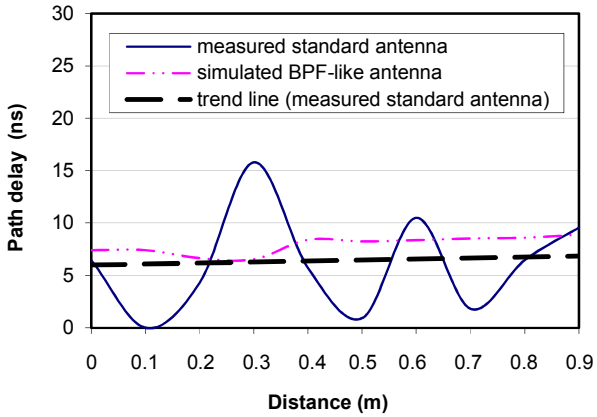
measured standard antenna
simulated BPF-like antenna
trend line (measured standard antenna)
Path delay (ns)
Distance (m)
30
25
20
15
10
5
0
0
0.1
0.2
0.3
0.4
0.5
0.6
0.7
0.8
0.9

(a)

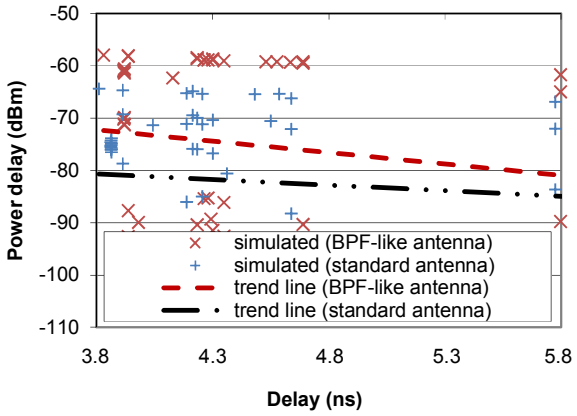
simulated (BPF-like antenna)
simulated (standard antenna)
trend line (BPF-like antenna)
trend line (standard antenna)
Power delay (dBm)
Delay (ns)
-50
-60
-70
-80
-90
-100
-110
3.8
4.3
4.8
5.3
5.8

(b)

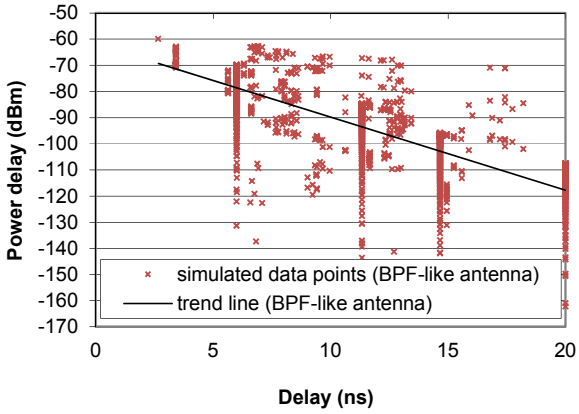
simulated data points (BPF-like antenna)
trend line (BPF-like antenna)
Power delay (dBm)
Delay (ns)
-50
-60
-70
-80
-90
-100
-110
-120
-130
-140
-150
-160
-170
0
5
10
15
20

(c)

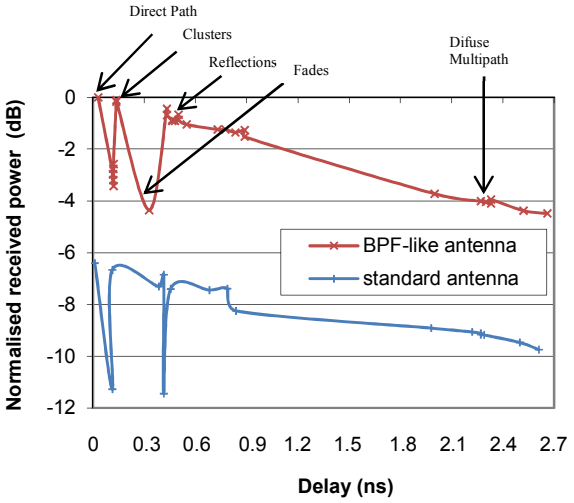

(d)

Figure 7 – (a) Simulated and measured path delay, (b) power delay profile for r = 0.9m, and (c) for r = 0m, and (d) simulated PDP impulse response

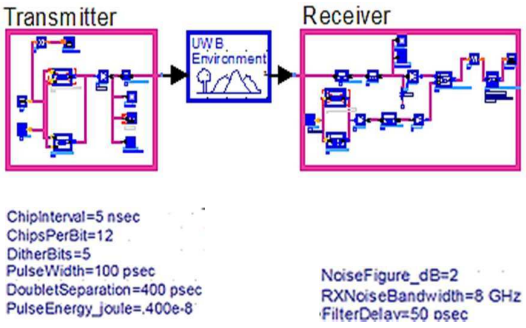

(a)

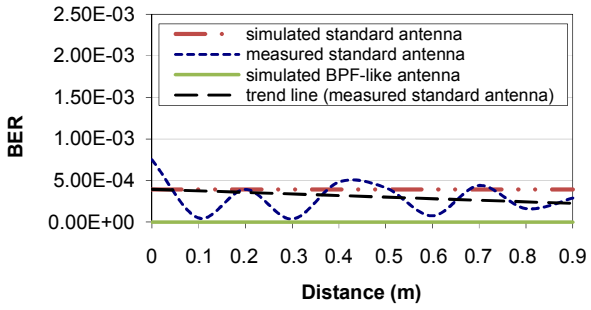

(b)

Figure 8 – (a) The UWB transceiver and the channel using ADS, (b) BER as a function of distance

Tables

Antenna parameters	Standard	BPF-like
Frequency (GHz)	2.9-4.8	3.2-4.8
Absolute gain (dBi) in isolation	2	2.3
Absolute gain (dBi) in proximity to plane A	3.8	7.1
VSWR (at lowest resonance) in proximity to plane A	2.757:1	3.57:1
S11 (dB) in proximity to plane A	-6.6	-5.2
Polarisation	horizontal	horizontal

Table 1 - Comparison between the antennas

Frequency	3.8 GHz
Cuboids resolution	10cm
Vertical plane angle resolution $\Delta\theta$	1º
Horizontal plane angle resolution $\Delta\varphi$	1º
Reflections	5
Transmitter Power	-43.42dBm

Table 2 - Parameters used in the Ray Launching simulator

RESPONSE TO THE REVIEWERS COMMENTS.

COM-2014-0057.R2
BPF-LIKE ANTENNA VALIDATION IN AN UWB IN-CAR WIRELESS CHANNEL

The authors would like to thank the Reviewers and Editor for their insightful suggestions. We have actioned all the points raised and amended the paper accordingly - the changes are given in red coloured text in the manuscript and detailed below.

Reviewer: 3

Comments to the Author
Good Job authors. Suggested corrections have been made.
Thanks.

Reviewer: 1

Comments to the Author
Thank you, I wish the author response on first comment could be added in the final revised version of the paper.
What I meant, on my last review, is that the pattern is not the key important element for such application.
Thanks. This is now reflected in the new version of the manuscript, thanks.

"Although the pattern of the BPF-like antenna was perceived beneficial (higher gains in the desired direction), this was not solely the important element for the application. Compared to the S11 response of the commercially available BPF, Fig. 2, the BPF-like antenna S11 is narrower in BW and therefore slightly improves rejection of the spectrum outside the actual BW. With a removed BPF, the BPF-like antenna provides comparable S11 performance to that of the commercial BPF and any possible spectrum beyond the antenna cut-off response (S11 = 0dB) is rejected by the amplifier´s inherent BW response."

"To compare the practice of the antennas fairly, unlike the BPF-like antenna, the standard antenna requires the BPF in place. Because the S11 of the former is -5dB and the latter -10dB, only when the BPF is in place, limits the link budget S21 by an inherent 2dB insertion loss of the filter, lower overall performance and is comparable to the BPF-like antenna for its validation in-car. "